Hydrogen and Halogen Bond Mediated Coordination Polymers of Chloro-Substituted Pyrazin-2-Amine Copper(I) Bromide Complexes

Aaron Mailman [1,*], **Rakesh Puttreddy** [1,2] , **Manu Lahtinen** [1] , **Noora Svahn** [1] and **Kari Rissanen** [1,*]

[1] Department of Chemistry, University of Jyväskylä, P.O. BOX 35, FI-40014 Jyväskylä, Finland; rakesh.puttreddy@tuni.fi (R.P.); manu.k.lahtinen@jyu.fi (M.L.); svahnnoora@gmail.com (N.S.)

[2] Faculty of Engineering and Natural Sciences, Tampere University, P. O. Box 541, FI-33101 Tampere, Finland

[*] Correspondence: aaron.m.mailman@jyu.fi (A.M.); kari.t.rissanen@jyu.fi (K.R.)

check for updates

Abstract: A new class of six mono- (**1**; 3-Cl-, **2**; 5-Cl-, **3**; 6-Cl-) and di-(**4**; 3,6-Cl, **5**; 5,6-Cl-, **6**; 3,5-Cl-) chloro-substituted pyrazin-2-amine ligands (**1–6**) form complexes with copper (I) bromide, to give 1D and 2D coordination polymers through a combination of halogen and hydrogen bonding that were characterized by X-ray diffraction analysis. These Cu(I) complexes were prepared indirectly from the ligands and $CuBr_2$ via an in situ redox process in moderate to high yields. Four of the pyrazine ligands, **1**, **4–6** were found to favor a monodentate mode of coordination to one Cu^I ion. The absence of a C6-chloro substituent in ligands **1**, **2** and **6** supported N1–Cu coordination over the alternative N4–Cu coordination mode evidenced for ligands **4** and **5**. These monodentate systems afforded predominantly hydrogen bond (HB) networks containing a catenated (μ_3-bromo)-Cu^I 'staircase' motif, with a network of 'cooperative' halogen bonds (XB), leading to infinite polymeric structures. Alternatively, ligands **2** and **3** preferred a μ_2-N,N' bridging mode leading to three different polymeric structures. These adopt the (μ_3-bromo)-Cu^I 'staircase' motif observed in the monodentate ligands, a unique single (μ_2-bromo)-Cu^I chain, or a discrete Cu_2Br_2 rhomboid (μ_2-bromo)-Cu^I dimer. Two main HB patterns afforded by self-complimentary dimerization of the amino pyrazines described by the graph set notation $R_2^2(8)$ and non-cyclic intermolecular N–H···N' or N–H···Br–Cu leading to infinite polymeric structures are discussed. The cooperative halogen bonding between C–Cl···Cl–C and the C–Cl···Br–Cu XB contacts are less than the sum of the van der Waals radii of participating atoms, with the latter ranging from 3.4178(14) to 3.582(15) Å. In all cases, the mode of coordination and pyrazine ring substituents affect the pattern of HBs and XBs in these supramolecular structures.

Keywords: hydrogen bond; halogen bond; pyrazine; chloropyrazine; chloropyrazin-2-amine; copper halide

1. Introduction

Construction of supramolecular structures from small molecules that self-assemble using hydrogen bonds (HBs) and other non-covalent interactions is the ultimate goal of the crystal engineering discipline [1]. Hydrogen bonding, due to the smaller size and easy polarizable nature of H-atom, has become a reliable tool to fabricate highly symmetric and exotic solid-state networks with tunable properties for applications in biology [2], and materials sciences [3]. The H-bonding knowledge gleaned from organic co-crystals have been applied to self-assemble metal-organic/coordination networks [4–7]. In fact, under the "crystal engineering umbrella", the design and synthesis of coordination compounds have received wide attention, due to their intriguing structural topologies [8–10]. Unlike organic

co-crystals, engineering inorganic compounds is dependent on two principals; primary coordination sphere (metal-ligand interactions) and secondary coordination sphere (non-covalent interactions) [11]. Despite several factors (e.g., pH, temperature) [12,13] could influence these two "parameters" for structurally diverse outcomes, modulation of networks based on the metal-ions geometry, organic ligands and their functional groups stand out in coordination chemistry research [14–21]. This fact is due to reproducible outcomes, that reflect the strong metal-ligand coordination bonds, and can be achieved with the judicious choice of organic ligands and metal-ions [14–21]. In this context, for example, O- and N-atoms are typical donors for the coordination bond formation; the former are derived from functional groups such as –COOH, –SO$_3$H and phosphonates [22–24], and the latter primarily from N-heterocycles [25]. The combined use of these two groups render ligands a strong coordinating ability, and are well-known for the preparation of homometallic and heterometallic coordination compounds [25].

In this regard, aminopyrazine carboxylic acids (L), of the forms L, and L$^+$, for the construction of hydrogen-bonded organic co-crystals [26–31], and L$^-$ functioning as a polydentate ligand in the preparation of coordination compounds [32–39] are reported in the literature. The presence of aromatic N-atoms and carboxylic acid/carboxylate groups within the same ligand may enhance the N–M bond strengths, often assisted by the polydentate bonding nature of O-atoms [26]. However, if the –COOH group is replaced by an aprotic donor substituent such as chlorine, and in combination with copper halides, what will happen to N-atom coordination nature? Will the chlorine substituents and metal-bound halides establish halogen bonds (XBs) [40–44], and halogen···halogen interactions [45–48]? This knowledge of XBs in metal complexes is derived from our previous experiences in halopyridine-Cu(I)/Cu(II) compounds [49–52]. When the bulky chlorines are installed close to an N-atom, can this affect the N–M coordination? How do the substituents mediate a hybrid topology containing –HN–H···N$_{pz}$ (pz = pyrazine) hydrogen bonds and C–Cl···Br halogen bonds? To test our hypothesis, we synthesized six chloro-substituted pyrazin-2-amine ligands (**1–6**) using procedures reported in the literature [53–57], and each ligand was combined with CuBr$_2$ in a 1:2 metal:ligand ratio. The CuBr complexes of these ligands were obtained by exploiting the known redox activity of Cu(II) halides in the presence of organic carbonyl compounds [31]. This work represents the first systematic study of the metal-ligand, HB, and XB interactions of chloro-substituted pyrazin-2-amines with copper halides and recent results will be discussed.

2. Materials and Methods

All reagents and solvents, including **2**, were obtained from commercial suppliers and were of at least reagent grade, and used as received, unless otherwise stated. The ligands **1** and **3–6** were prepared by modified literature procedures [53–58]. Full experimental, FT-IR spectroscopic details and the single-crystal [59–66] and powder X-ray experimental [67–69], and structure refinements for **1**·CuBr–**6**·CuBr (CCDC numbers: 2001484–2001491) are given in the Supporting Information.

3. Results and Discussion

This new class of chloro-substituted pyrazin-2-amine ligands given in Chart 1 were made to react with cupric bromide (CuBr$_2$), either by refluxing in a 1:1:1 (*v/v/v*) mixture of acetone (Ace), ethanol (EtOH) and acetonitrile (MeCN) or 1:5 (*v/v*) mixture of Ace:EtOH to afford the desired Cu(I)Br complexes, via an in situ redox process, according to Scheme 1. An excess of pyrazine ligand was used to act as ligand and auxiliary base for the HBr liberated during the reduction of CuBr$_2$ to CuBr by acetone [70]. The reduction was accompanied by a color change from a deep blue-green solution characteristic of Cu(II) ions, to a clear, yellow solution upon refluxing for several minutes. In total, eight different Cu(I)Br coordination complexes obtained from the combination of these six ligands will be discussed.
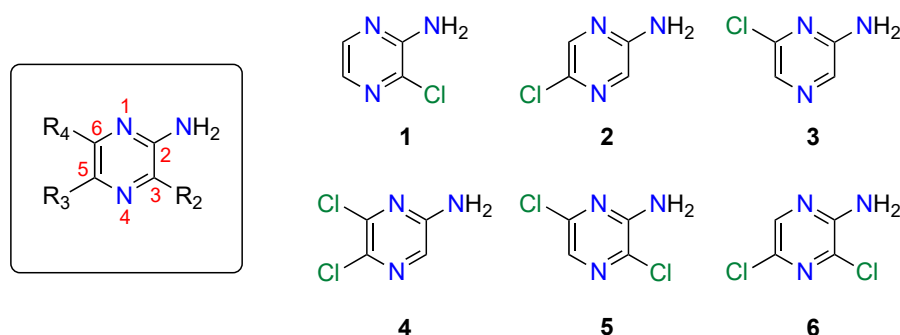
Chart 1. List of chloro-substituted pyrazin-2-amines and numbering scheme used throughout: 2-amino-3-chloropyrazine (**1**), 2-amino-5-chloropyrazine (**2**), 2-amino-6-chloropyrazine (**3**), 2-amino-5,6-dichloropyrazine (**4**), 2-amino-3,6-dichloropyrazine (**5**), and 2-amino-3,5-dichloropyrazine (**6**).
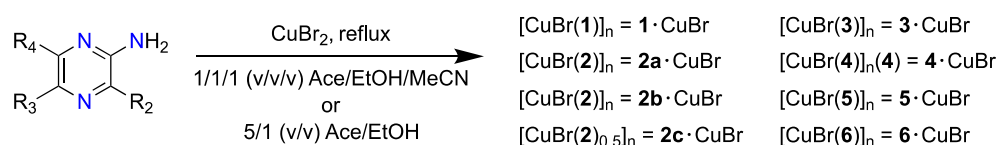
Scheme 1. General synthetic route to Cu(I)-complexes of ligands **1–6** via an in situ redox process from $CuBr_2$, and the nomenclature used.

X-ray quality crystals of the complexes were obtained by slowly concentrating the reaction mixtures by controlled evaporation. Interestingly, **2c**·CuBr was only obtained from a 1:5 (*v/v*) Ace and EtOH reaction mixture, together with **2b**·CuBr. The concomitant polymorphism did not allow the isolation of **2c**·CuBr as a phase pure material; however, **2b**·CuBr could be prepared independently by alternative methodologies in moderate yield. Moreover, attempts to recrystallize the mixture of **2c**·CuBr and **2b**·CuBr from MeCN afforded only complexes **2a**·CuBr and **2b**·CuBr. This suggests the **2c**·CuBr is only somewhat stable when prepared from a 1:5 (*v/v*) Ace:EtOH mixture and readily dissociates in the polar aprotic solvent MeCN. Optical microscopy could be routinely used to distinguish the different color and crystal habits of the three different polymorphs of (**2a–c**) CuBr (See Figure S1). Powder X-ray diffraction methods were used to demonstrate the solid-state structures and estimate the phase purity of the bulk material by using Pawley full pattern fittings. The FT-IR spectra of the isolated complexes were compared to the respective ligands, and display two specific regions from 3500–2800 cm^{-1} and 1200–400 cm^{-1} for the hydrogen-bonded N–H stretching [71] and fingerprint regions, respectively, which are distinctive for each ligand and complex (see Figures S10–S16).

In general, reactions between donor ligands (L) and CuX (X = Cl, Br, I) yield complexes with formula $Cu_nX_nL_m$, that display diverse structural topologies, containing rhomboid dimer, zigzag polymer, staircase polymer, closed cubane, and hexagon clusters, have been reported in the literature [72]. The structural diversification stems from the very nature of the ligand coordination modes and the tendency of copper halides to form clusters via μ_2- and μ_3-halide bridges [73]. In our eight complexes, we obtained three topologies exclusively, namely staircase polymer (**1**·CuBr, **2a**·CuBr, **2c**·CuBr, **4**·CuBr, **5**·CuBr, and **6**·CuBr), rhomboid dimer (**2b**·CuBr), and zigzag polymer (**3**·CuBr), as depicted in Figure 1. The staircase and rhomboid structures feature well-known Cu···Cu distances (Cuprophilic interactions) [74], ranging from 2.7547(13) to 3.086(4) Å, but will not be discussed further in the text.

The complexes **1**·CuBr and **2a**·CuBr both crystallize as clear, pale-yellow or colorless needles in an orthorhombic space group, *Pna*2$_1$ and *P*2$_1$2$_1$2$_1$, respectively. Both contain discrete 1D polymeric chains of the catenated (μ_3-bromo)-Cu^I 'staircase' that run parallel to the *c*-axis and *a*-axis in **1**·CuBr and **2a**·CuBr, respectively. In these chains, the Cu(I) ions have tetrahedral geometry, coordinated by

three bromines and the pyrazine N1-atom. Since the pyrazine N4-atom is not involved in the N–Cu bond formation, it plays a central role in the HB formation involving a C2-amino group of an adjacent chain. The orthogonal arrangement of the discrete 1-D polymeric chains leads to a herringbone packing structure in both **1**·CuBr and **2a**·CuBr, as illustrated in Figure 2. The N4···H–N HBs in **1**·CuBr of 2.245(11) Å, [∠N4···H–N = 155.6(9)°] are shorter than in **2a**·CuBr [2.349(7) Å, ∠N4···H–N = 133.4(5)°]. The XBs in **1**·CuBr and **2a**·CuBr complexes are, however, more comparable at 3.465(3) Å [∠Br···Cl–C = 165.4(3)°] and 3.509(3) Å [∠Br···Cl–C = 159.5(3)°], respectively. This network of HBs and XBs does lead to a complex molecular packing that extends in three dimensions.
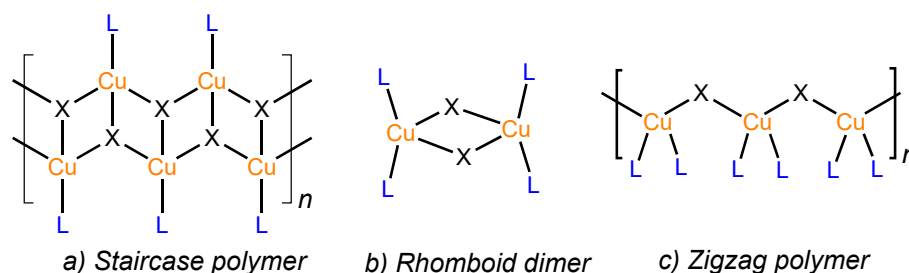
**Figure 1.** The three structural topologies realized in the Cu(I)-complexes of **1–6**, (**a**) catenated (μ_3-bromo)-Cu^I 'staircase' polymer, (**b**) Cu$_2$Br$_2$ rhomboid (μ_2-bromo)-Cu^I dimers, and (**c**) zigzag polymer (μ_2-bromo)-Cu^I chains.

The complex **6**·CuBr crystallizes in a monoclinic *P*2$_1$/*c* space group, and is composed of 1D polymeric chains of the catenated (μ_3-bromo)-Cu^I 'staircase' that run along the shortest unit cell *a*-axis. The asymmetric unit contains one bromide anion and a one Cu(I) cation coordinated by the sterically less hindered N1-atom of **6**. Not surprisingly, the C3 and C5 chloro-substituents vicinal to the N4-atom render this ring nitrogen Cu-coordination passive. The orthogonal arrangement of the discrete 1D polymeric chains leads to a herringbone packing structure that is similar to **1**·CuBr and **2a**·CuBr (for **6**·CuBr, see Figure S2). The 1D chains are aligned by a more extensive network of XBs, afforded by the C3- and C5-Cl substituents (C3–Cl···Br–Cu [3.4794(14) Å, ∠Br···Cl–C = 162.44(19)°], C5–Cl···Br–Cu [3.4178(14) Å, ∠Br···Cl–C = 175.34(19)°]) and longer N4···H–N of 2.511(4) Å, [∠N4···H–N = 135.8(3)°] HBs, compared to **1**·CuBr and **2a**·CuBr.

The N1–Cu mode of coordination realized in **1**·CuBr, **2a**·CuBr, and **6**·CuBr allows the vicinal C2-amino group hydrogen and a Cu(I) bound bromide to form cyclic N–H···Br–Cu HBs, with distances varying from ca. 2.609(7)–2.774(2) Å [∠Br···H–N = 146(1)°–168.9(4)°], within the discrete polymeric (μ_3-bromo)-Cu^I 'staircase' chain (See Figure S3). These cyclic intra-chain N–H···Br HBs afford a pseudo-helical type arrangement of the pyrazine ligands along the polymeric (μ_3-bromo)-Cu^I 'staircase' backbone. The HBs, in combination with the C–Cl···Br–Cu XBs from neighboring chains, aids the stabilization of the catenated (μ_3-bromo)-Cu^I 'staircase' polymeric chains in these complexes.

The complexes **4**·CuBr and **5**·CuBr crystallize in a triclinic *P*-1 and monoclinic *P*2$_1$/n space groups, respectively. In both complexes, the catenated (μ_3-bromo)-Cu^I 'staircase' motif is preserved, however, the tetrahedral Cu(I) centers are coordinated by three bromides and a pyrazine N4-atom. In the case of **4**·CuBr, it crystallizes with an additional pyrazine molecule in the asymmetric unit that is not involved in coordination with the Cu(I) centers. The N4–Cu coordination mode found in both complexes allows the C2-amino group to participate in hydrogen-bonding with a neighboring pyrazine in a self-complimentary N–H···N$_{pz}$ pyrazine dimer. The resultant hydrogen-bonded dimers in **4**·CuBr and **5**·CuBr are described by the graph set notation R$_2^2$(8), with HB parameters of ca. 2.308(12) Å, [166.4(7)°] and 2.138(5) Å [160.1(3)°], respectively (Figure 3). These Watson–Crick-like base pairing structures are characteristic of aminopyrazine derivatives [75,76]. The R$_2^2$(8) hydrogen bonding in **4**·CuBr and **5**·CuBr leads to essentially linear chains that pack into laminar 2D polymeric sheets held together by the polymeric (μ_3-bromo)-Cu^I 'staircase' motif. The non-coordinating pyrazine in **4**·CuBr forms an additional set of R$_2^2$(8) hydrogen-bonded dimers that cross-link the 2D sheets via non-cyclic

N–H···N-ring hydrogen bonds [2.219(11) Å ∠N–H···N4, 177.7(8)°], into a 3D structure shown in Figure 3a. Although **4**·CuBr and **5**·CuBr lack the intra-chain cyclic N–H···Br–Cu HBs (see Figure S4) found in **1**·CuBr, **2a**·CuBr, and **6**·CuBr, a network of non-cyclic inter-chain N–H···Br–Cu and C–H···Br–Cu HBs are established between neighboring chains in **5**·CuBr or the non-complexed pyrazine in **4**·CuBr. Overall, the N–H···Br–Cu and C–H···Br–Cu HBs together with the C–Cl···Br–Cu, and C–Cl···Cl–C XBs stabilize the polymeric μ₃-bromo 'staircase', and further cross-link the laminar 2D polymeric sheets into complex 3D structures. Notwithstanding the structural similarities between **4**·CuBr and **5**·CuBr, as determined by single-crystal X-ray diffraction, the solid-state structure of **4**·CuBr could not be demonstrated in the bulk material, as determined by powder X-ray diffraction. Full pattern Pawley analysis of **4**·CuBr suggests that the bulk material is effectively isomorphous with **6**·CuBr (See Table S6 and Figure S8). This suggests that additional polymorphs may exist where the Cu(I) center is coordinated by the sterically more congested N1 in **4**. This possibility has also been observed in **3**·CuBr, and polymorphism has been demonstrated in **2(a–c)**·CuBr, as described below. Despite repeated attempts, under different conditions, alternative single-crystal structures of Cu(I) complexes of **4** have still not been realized.
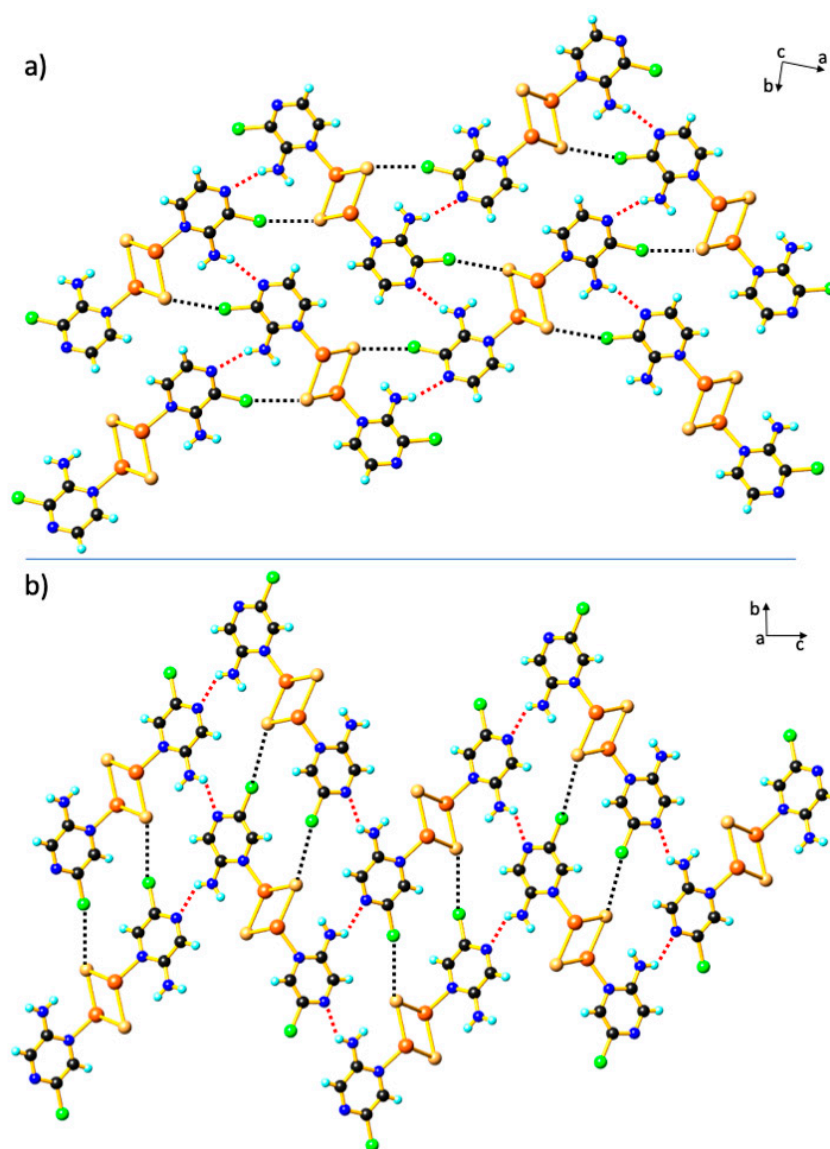

Figure 2. The herringbone packing arrangement of the discrete 1D polymeric chains of (**a**) **1**·CuBr, (**b**) and **2a**·CuBr. The red- and black- dotted lines represent hydrogen and halogen bonds, respectively.
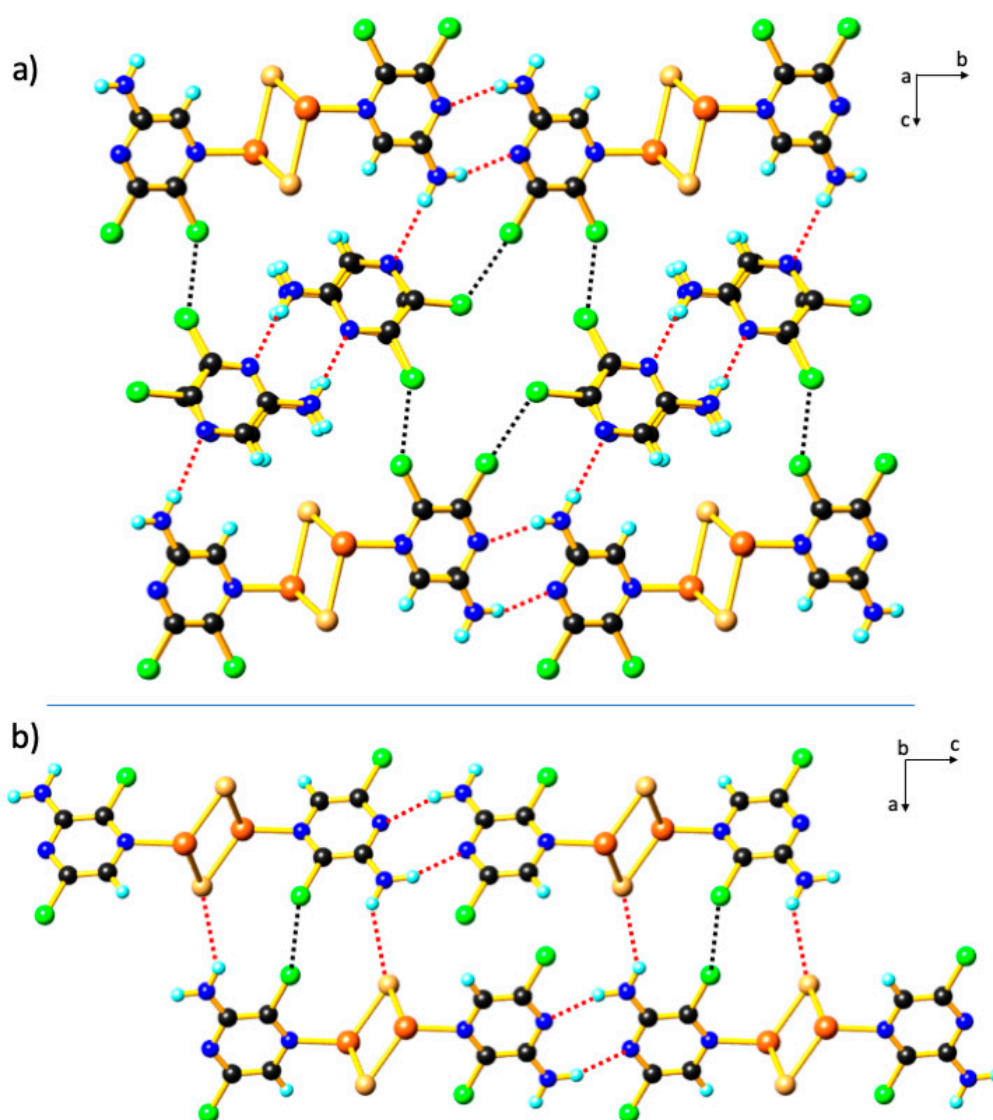
Figure 3. The $R_2^2(8)$ hydrogen-bonded ring motif realized in the crystal packing of (**a**) **4**·CuBr, and (**b**) **5**·CuBr. Red dotted lines are N–H···N $R_2^2(8)$ and N–H···Br–Cu hydrogen bonds, and black are C–Cl···Cl–Cu halogen bonds.

The three polymeric structures **2b**, **2c**·and **3**·CuBr all contain bridging μ_2-*N,N′* pyrazine ligands, and display the three (CuBr)$_n$ structural motifs outlined in Figure 1. Complex **2b**·CuBr crystallizes in the orthorhombic space group *Pbcn* as amber, prismatic blocks (See Figure S1a). In this complex, the pyrazine ligands are μ_2-*N,N′* bridging between Cu$_2$Br$_2$ rhomboid dimer units to afford a distorted tetrahedral coordination geometry at the Cu(I) ion formed by two symmetry-equivalent bromines, and the N1- and N4-atoms of two different pyrazine ligands. This leads to a 2D dimensional honey-comb sheet that propagates in the *ab* plane, as illustrated in Figure 4a. The honey comb structure is similar to the [CuCl(μ-2,5-dimethylpyrazine-*N,N′*)]$_n$ structure reported in the literature [77]. Adjacent layers are held together by C5–Cl···Br–Cu [3.5105(7) Å, ∠Br···Cl–C = 161.83(8)°] XBs and N–H···Br–Cu [2.6402(2) Å, ∠Br···H–N = 159.28(14)°] HBs, as given in Figure 4b. Moreover, these HBs and XBs, together with steric effects, prevent the formation of a catenated μ-bromo-Cu^I motif, as in the staircase polymers previously mentioned.
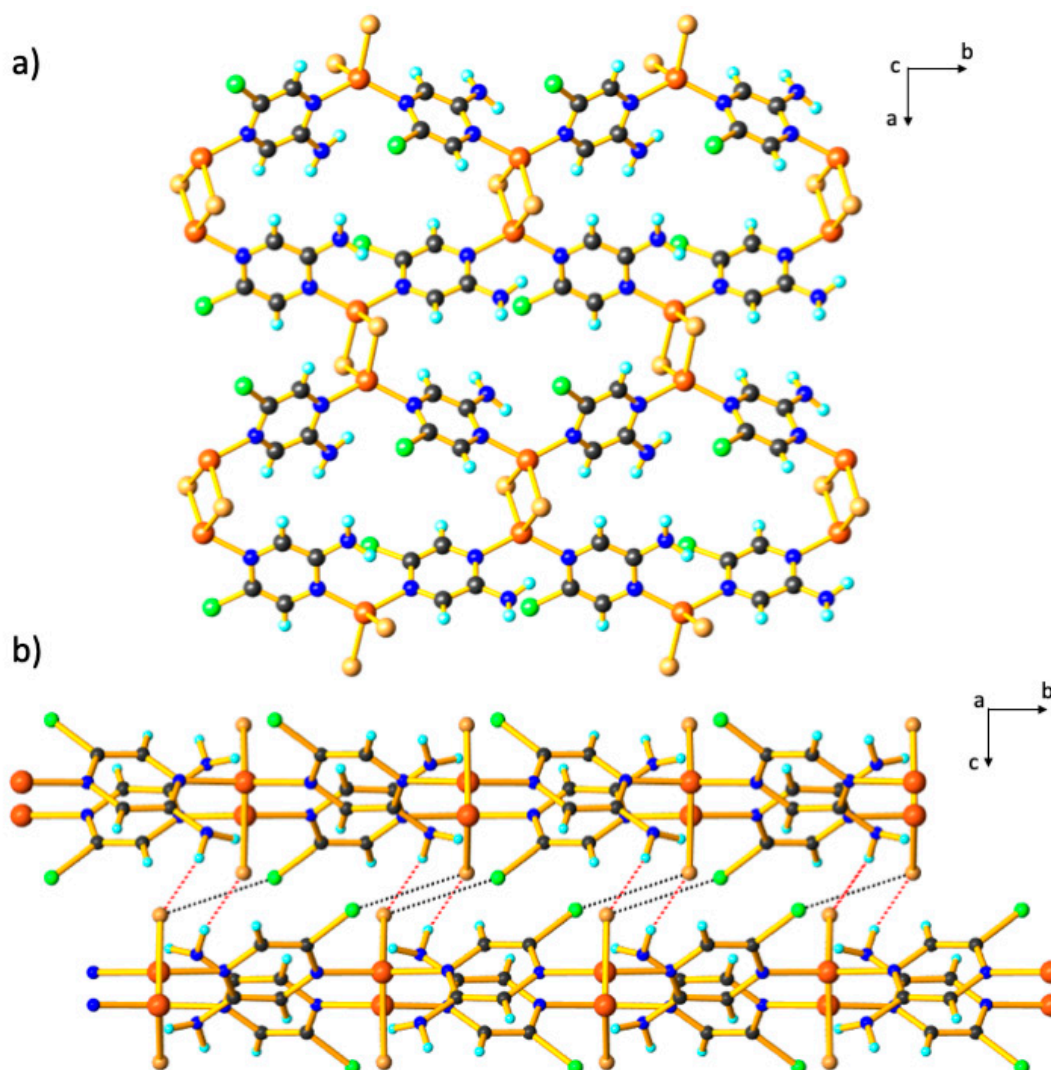
Figure 4. (**a**) 2-D Honey comb motif of **2b**·CuBr, and (**b**) 3-D packing unit displaying hydrogen (red dotted lines) and halogen bonds (black dotted lines) between 2-D sheets.

The bright yellow, needles of **2c**·CuBr crystallize in the monoclinic space group $P2_1/n$. The asymmetric unit consists of a Cu(I) ion; one bromide and one half of a pyrazine ligand. The C5-chlorine and C2-amine substituents exhibit a positional disorder with 50:50 occupancies. The distorted tetrahedral coordination environment of Cu(I) consists of one pyrazine nitrogen and three symmetry equivalent bromide anions. Ligand **2** is μ_2-*N,N'* bridging to yield a 2D polymeric sheet containing the catenated (μ_3-bromo)-Cu^I 'staircase' chain structure, as shown in Figure 5. The polymeric structure of **2c**·CuBr is similar to that found in the 2D coordination polymer of 2-aminopyrazine with CuI (i.e., [Cu$_2$I$_2$(2-aminopyrazine)]$_n$) [78] and [2(μ-2,5-dimethylpyrazine-*N,N'*)Cu$_2$]$_n$ where X = Br, I [77]. The adjacent sheets are linked by N–H···Br–Cu [2.6054(17) Å, ∠Br···H–N = 175(4)°] interactions between the C2-amino group and a Cu(I)-bound bromide. As a result of positional disorder, the C–Cl bond length associated with the 50% occupancy is close to the standard C–Cl bond distance, and results in a weak C5–Cl···Br–Cu [3.582(15) Å, ∠Cl···Br–Cu = 103.9(9)°] 'contact'. These weak interactions are likely triggered by the N–H···Br–Cu interactions between the neighboring molecules in this laminar structure. Due to the disorder, there are possible HB and XB interactions that could alternate along a plane that passes through the amino- and chloro-substituents of the pyrazines of adjacent sheets, thus forming moderately short Cl···Cl halogen contacts with R$_{XB}$ = 0.88. These HBs and XB interactions

further supports the catenated (μ_3-bromo)-Cu^{I} 'staircase' motif as a common structural feature in these complexes.
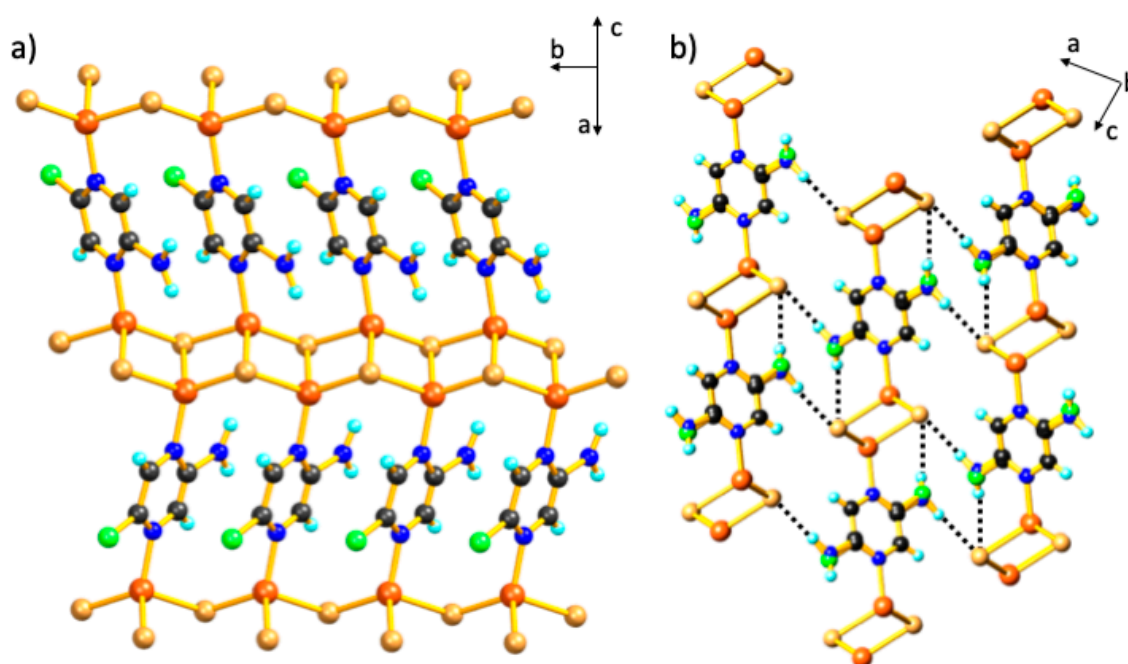
Figure 5. (**a**) Here, 2D polymeric sheet structure of **2c**·CuBr, and (**b**) the hydrogen and halogen bonds (black dotted lines) between sheets in the laminar structure. Note: the disordered atoms were not omitted to reflect the discussion.

The complex **3**·CuBr, crystallized in the monoclinic space group $P2_1/n$. The distorted tetrahedral coordination environment of the Cu(I) is composed of two symmetry-related bromides and two crystallographically different N-atoms from two distinct pyrazine ligands. The Cu(I) ions are bridged by μ_2-*N*,*N'* pyrazine ligands, forming 1D linear chains that run along the *c*-axis as illustrated in Figure 6a. These chains are further linked into a 2D sheet structure by polymeric (μ_2-bromo)-Cu^{I}-Br chains along the *a*-axis. The 2D layers are not flat, but instead adopt a slightly corrugated pattern because of the ∠N–Cu–N = 136.6(4)° at the distorted tetrahedron at the Cu(I) ion, as shown in Figure 6b. Two types of interactions assemble the layers into a 3D structure. First is the hydrogen bonding between a C2-amino group and Cu(I)-bound bromide from an adjacent layer [2.3615(10) Å, ∠Br···H–N = 164.2 (7)°; 2.4846(12) Å, ∠Br···H–N = 158.9(6)°], to afford a $R_2^2(8)$ ring motif from a set of two N–H···Br HBs. The second interaction is C6–Cl···Br–Cu halogen bonds [3.527(3) Å, ∠Br···Cl–C = 158.8(4)°] between a chlorine on the pyrazine ring and bromide coordinated to Cu(I) on an adjacent layers, as shown in Figure 6b. Similar to the (μ_3-bromo)-Cu^{I} 'staircase' motif, the μ_2-bromo polymeric chains found in **3**·CuBr is fully stabilized by the network of HB and XBs, and is likely adopted because of the steric demands of the N1 coordination, compared to the more accessible N4-coordination mode in ligand **3**.
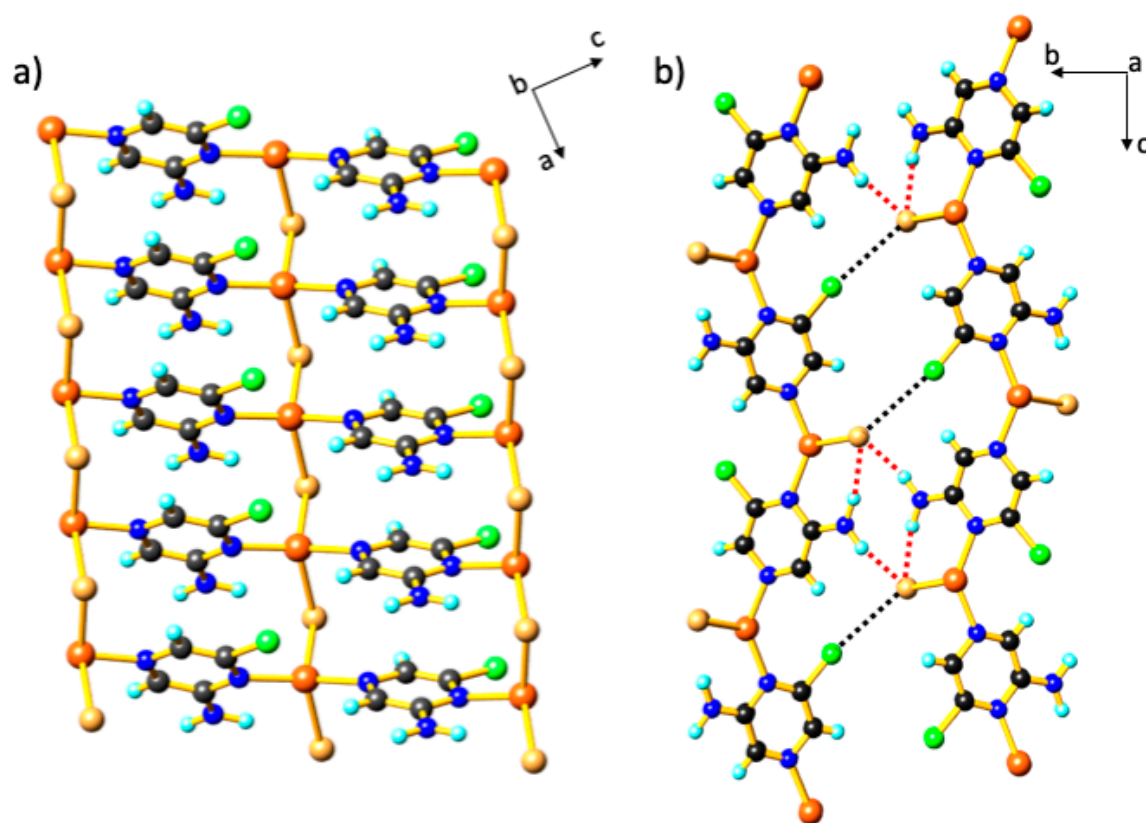
Figure 6. (**a**) Here, 2D Layered structure of **3**·CuBr, and (**b**) 2-D layers stack viewed along the a-axis. Red dotted lines are N–H···Br–Cu hydrogen bonds, and black are C6–Cl···Br–Cu halogen bonds.

4. Conclusions

In summary, eight Cu(I)Br coordination polymers have been synthesized, and their single-crystal structures characterized by using X-ray diffraction analysis. Three different types of (CuBr)$_n$ arrangements with n ≥ 2 were realized. Six of the eight complexes form characteristic catenated μ_2-bromo staircase polymers that are reminiscent of those reported in related copper(I) halide complexes. Our findings indicate that a combination of cyclic and non-cyclic hydrogen bonds (HBs), between the C2-amino group and Cu(I) bound bromides (N–H···Br–Cu) and halogen bonding (C–Cl···Br–Cu) interactions, underpins the formation of catenated μ_2- and μ_3-bromo (CuBr)$_n$ polymeric structures.

It was found that the mode of coordination by the dichloro-substituted aminopyrazines **4**–**6** to the Cu(I) could be readily predicted based on simple electronic and steric arguments. In the mono chloro-substituted pyrazines **1**–**3**, these effects were less obvious, as evidenced by the realization of both monodentate (**1**·CuBr and **2a**·CuBr), and polymeric structures (**2b**·CuBr, **2c**·CuBr and **3**·CuBr). The polymeric **3**·CuBr suggests that there is little steric hindrance afforded by the combination of a C2-amino and C6-chloro substituents vicinal to the N1–Cu coordination site, and may indicate that this is not a major factor in determining N1-Cu coordination passiveness in **4**·CuBr and **5**·CuBr. This could also account for the unique polymeric (μ_2-bromo)-Cu^I chain in **3**·CuBr, which is able to accommodate the more sterically demanding N1–Cu coordination, and allows stabilizing cyclic N–H···Br HBs.

Three polymorphs were isolated and structurally characterized based on the simple 2-amino-5-chloropyrazine ligand, **2**. We demonstrate that concomitant polymorphism leads to both 1D and 2D polymeric structures based on the μ_3-bromo staircase polymer motif in **2a**·CuBr and **2c**·CuBr, respectively. The third polymorph, **2b**·CuBr, displays a unique honeycomb network composed of discrete Cu$_2$Br$_2$ rhomboid (μ_2-bromo)-Cu^I dimers and μ_2-*N,N'* bridging ligands. These three polymorphs demonstrate the role of the C2-amino group in forming three types of hydrogen bonding patterns recognized in all eight of these complexes. The self-complementary, symmetry-related N–H···N$_{pz}$ pyrazine dimers

described by the graph set notation $R_2^2(8)$ with distances varying from ca. 2.138(5)–2.308(12) Å [∠Br···H–N = 160.1(3)°–177.7(8)°] were found in N4–Cu coordination structures **4**·CuBr and **5**·CuBr, and resulted in the formation of laminar 2D sheet structures. Based on the competitive binding sites in the simple mono-substituted aminopyrazine ligands, and the role of the amino-group to influence structural features through hydrogen bonding, we are currently investigating the formation of dihalopyrazine-copper complexes.

The Cu(I) halide complexes have attracted considerable attention because of their physical properties and functional applications in future technologies, such as solar energy conversion, light emitting devices, and possible sensing applications. As a result, there has been considerable focus on exploring and developing structural relationships that will provide insights for future materials design and synthesis. The interesting 2D-honeycomb network found in **2b**·CuBr is a particularly appealing architecture that could have applications in gas storage or separation, if the porosity can be tuned through ligand design. While systematic structural studies on Cu(I) halide and pyrazine derivatives have not received much attention to date, this work demonstrates a level of structural predictability not typically observed in Cu(I) halide complexes. We believe future investigations of halo-substituted aminopyrazines and related pyrazine derivatives will provide the basis for an empirical structural database that will aid future material designs.

Supplementary Materials: The following are available online at http://www.mdpi.com/2624-8549/2/3/45/s1, Full experimental, the single-crystal experimental and CCDC number details for **1**·CuBr–**6**·CuBr (Tables S1–S3), structure refinements for **1**·CuBr–**6**·CuBr, crystal habits of **2(a,b,c)**·CuBr (Figure S1), powder X-ray diffraction analysis (Tables S4–S6, Figures S5–S9), FT-IR spectroscopic details (Figures S10–S16), and X-ray crystal figures (Figures S2–S4).

Author Contributions: The manuscript was written and edited through the contributions of all authors. R.P. and A.M. were responsible for the original concept, methodology development and SCXRD analysis. The ligand synthesis was carried out by N.S., while the PXRD data collection, analysis and Pawley fittings were performed by M.L. K.R. and A.M. were responsible for proof reading and the final manuscript version. All authors have read and agreed to the published version of the manuscript.

Conflicts of Interest: The authors declare no conflict of interest.

Reference and Note

1. Desiraju, G.R.; Vittal, J.J.; Ramanan, A. *Crystal Engineering: A Textbook*; World Scientific: Singapore, 2011.
2. Jeffrey, G.A.; Saenger, W. *Hydrogen Bonding in Biological Structures*; Springer: Berlin/Heidelberg, Germany, 1991.
3. Amabilino, D.B.; Smith, D.K.; Steed, J.W. Supramolecular materials. *Chem. Soc. Rev.* **2017**, *46*, 2404–2420. [CrossRef] [PubMed]
4. Biradha, K.; Desiraju, G.R.; Braga, D.; Grepioni, F. Hydrogen Bonding in Organometallic Crystals. 3.1 Transition-Metal Complexes Containing Amido Groups. *Organometallics* **1996**, *15*, 1284–1295. [CrossRef]
5. Brammer, L.; Rivas, J.C.M.; Atencio, R.; Fang, S.; Pigge, F.C. Combining hydrogen bonds with coordination chemistry or organometallic π-arene chemistry: Strategies for inorganic crystal engineering. *J. Chem. Soc. Dalton Trans.* **2000**, 3855–3867. [CrossRef]
6. Beatty, A.M. Hydrogen bonded networks of coordination complexes. *CrystEngComm* **2001**, *3*, 243–255. [CrossRef]
7. Epstein, L.M.; Shubina, E.S. New types of hydrogen bonding in organometallic chemistry. *Coord. Chem. Rev.* **2002**, *231*, 165–181. [CrossRef]
8. Nair, K.P.; Pollino, J.M.; Weck, M. Noncovalently Functionalized Block Copolymers Possessing Both Hydrogen Bonding and Metal Coordination Centers. *Macromolecules* **2006**, *39*, 931–940. [CrossRef]

9. Chandrasekhar, P.; Mukhopadhyay, A.; Savitha, G.; Moorthy, J.N. Orthogonal self-assembly of a trigonal triptycene triacid: Signaling of exfoliation of porous 2D metal–organic layers by fluorescence and selective CO2 capture by the hydrogen-bonded MOF. *J. Mater. Chem. A* **2017**, *5*, 5402–5412. [CrossRef]

10. Aakeroy, C.B.; Beatty, A.M. Solid State, Crystal Engineering and Hydrogen Bonds. *ChemInform* **2004**, *35*. [CrossRef]

11. Cook, S.A.; Borovik, A.S. Molecular Designs for Controlling the Local Environments around Metal Ions. *Acc. Chem. Res.* **2015**, *48*, 2407–2414. [CrossRef]

12. Friese, V.A.; Kurth, D.G. Soluble dynamic coordination polymers as a paradigm for materials science. *Coord. Chem. Rev.* **2008**, *252*, 199–211. [CrossRef]

13. Seetharaj, R.; Vandana, P.V.; Arya, P.; Mathew, S. Dependence of solvents, pH, molar ratio and temperature in tuning metal organic framework architecture. *Arab. J. Chem.* **2019**, *12*, 295–315. [CrossRef]

14. Zhu, R.; Lübben, J.; Dittrich, B.; Clever, G.H. Stepwise Halide-Triggered Double and Triple Catenation of Self-Assembled Coordination Cages. *Angew. Chem. Int. Ed.* **2015**, *54*, 2796–2800. [CrossRef]

15. Sun, Q.-F.; Iwasa, J.; Ogawa, D.; Ishido, Y.; Sato, S.; Ozeki, T.; Sei, Y.; Yamaguchi, K.; Fujita, M. Self-Assembled M24L48 Polyhedra and Their Sharp Structural Switch upon Subtle Ligand Variation. *Science* **2010**, *328*, 1144–1147. [CrossRef]

16. Schultz, A.; Li, X.; Barkakaty, B.; Moorefield, C.N.; Wesdemiotis, C.; Newkome, G.R. Stoichiometric Self-Assembly of Isomeric, Shape-Persistent, Supramacromolecular Bowtie and Butterfly Structures. *J. Am. Chem. Soc.* **2012**, *134*, 7672–7675. [CrossRef]

17. Li, S.; Moorefield, C.N.; Wang, P.; Shreiner, C.D.; Newkome, G.R. Self-Assembly of Shape-Persistent Hexagonal Macrocycles with Trimeric Bis(terpyridine)–FeII Connectivity. *Eur. J. Org. Chem.* **2008**, *2008*, 3328–3334. [CrossRef]

18. Tominaga, M.; Suzuki, K.; Kawano, M.; Kusukawa, T.; Ozeki, T.; Sakamoto, S.; Yamaguchi, K.; Fujita, M. Finite, Spherical Coordination Networks that Self-Organize from 36 Small Components. *Angew. Chem. Int. Ed.* **2004**, *43*, 5621–5625. [CrossRef]

19. Ronson, T.K.; Fisher, J.; Harding, L.P.; Rizkallah, P.J.; Warren, J.E.; Hardie, M.J. Stellated polyhedral assembly of a topologically complicated Pd4L4 'Solomon cube'. *Nat. Chem.* **2009**, *1*, 212–216. [CrossRef]

20. Olenyuk, B.; Whiteford, J.A.; Fechtenkötter, A.; Stang, P.J. Self-assembly of nanoscale cuboctahedra by coordination chemistry. *Nature* **1999**, *398*, 796–799. [CrossRef]

21. Song, B.; Kandapal, S.; Gu, J.; Zhang, K.; Reese, A.; Ying, Y.; Wang, L.; Wang, H.; Li, Y.; Wang, M.; et al. Self-assembly of polycyclic supramolecules using linear metal-organic ligands. *Nat. Commun.* **2018**, *9*, 4575. [CrossRef]

22. Zhang, J.-W.; Kan, X.-M.; Li, X.-L.; Luan, J.; Wang, X.-L. Transition metal carboxylate coordination polymers with amide-bridged polypyridine co-ligands: Assemblies and properties. *CrystEngComm* **2015**, *17*, 3887–3907. [CrossRef]

23. Ali Akbar Razavi, S.; Morsali, A. Linker functionalized metal-organic frameworks. *Coord. Chem. Rev.* **2019**, *399*, 213023. [CrossRef]

24. Goura, J.; Chandrasekhar, V. Molecular Metal Phosphonates. *Chem. Rev.* **2015**, *115*, 6854–6965. [CrossRef]

25. Lawrance, G.A. Mixed Donor Ligands Based in part on the article Mixed Donor Ligands by Nikolay N. Gerasimchuk & Kristin Bowman-James which appeared in the Encyclopedia of Inorganic Chemistry, First Edition. Available online: https://doi.org/10.1002/9781119951438.eibc0132 (accessed on 15 December 2011).

26. Taghipour, F.; Mirzaei, M. A survey of interactions in crystal structures of pyrazine-based compounds. *Acta Crystallogr. Sect. C* **2019**, *75*, 231–247. [CrossRef] [PubMed]

27. Wang, Y.; Stoeckli-Evans, H. The inner-salt zwitterion, the dihydrochloride dihydrate and the dimethyl sulfoxide disolvate of 3,6-bis(pyridin-2-yl)pyrazine-2,5-dicarboxylic acid. *Acta Crystallogr. Sect. C* **2012**, *68*, o431–o435. [CrossRef]

28. Dobson, A.J.; Gerkin, R.E. 3-Aminopyrazine-2-carboxylic Acid. *Acta Crystallogr. Sect. C* **1996**, *52*, 1512–1514. [CrossRef] [PubMed]

29. Berrah, F.; Bouacida, S.; Roisnel, T. 2-Amino-3-carboxypyrazin-1-ium dihydrogen phosphate. *Acta Crystallogr. Sect. E* **2011**, *67*, o1409–o1410. [CrossRef] [PubMed]

30. Berrah, F.; Ouakkaf, A.; Bouacida, S.; Roisnel, T. Bis(2-amino-3-carboxypyrazin-1-ium) sulfate dihydrate. *Acta Crystallogr. Sect. E* **2011**, *67*, o677–o678. [CrossRef] [PubMed]

31. Berrah, F.; Bouacida, S.; Bouhraoua, A.; Roisnel, T. 2-Amino-3-carboxypyrazin-1-ium perchlorate bis(2-aminopyrazin-1-ium-3-carboxylate) monohydrate. *Acta Crystallogr. Sect. E* **2012**, *68*, o1714–o1715. [CrossRef]

32. Barszcz, B.; Masternak, J.; Hodorowicz, M.; Jabłońska-Wawrzycka, A. Cadmium(II) and calcium(II) complexes with N,O-bidentate ligands derived from pyrazinecarboxylic acid. *J. Therm. Anal. Calorim.* **2012**, *108*, 971–978. [CrossRef]

33. Goher, M.A.S.; Al-Salem, N.A.; Mautner, F.A.; Klepp, K.O. A copper(II) azide compound of pyrazinic acid containing a new dinuclear complex anion $[Cu_2(N_3)_6]_2^-$. Synthesis, spectral and study of KCu_2(pyrazinato) $(N_3)_4$. *Polyhedron* **1997**, *16*, 825–831. [CrossRef]

34. Zheng, X.; Chen, Y.; Ran, J.; Li, L. Synthesis, crystal structure, photoluminescence and catalytic properties of a novel cuprous complex with 2,3-pyrazinedicarboxylic acid ligands. *Sci. Rep.* **2020**, *10*, 6273. [CrossRef] [PubMed]

35. Li, Y.-W.; Tao, Y.; Hu, T.-L. Synthesis, structure, and photoluminescence of ZnII and CdII coordination complexes constructed by structurally related 5,6-substituted pyrazine-2,3-dicarboxylate ligands. *Solid State Sci.* **2012**, *14*, 1117–1125. [CrossRef]

36. Bouchene, R.; Khadri, A.; Bouacida, S.; Berrah, F.; Merazig, H. Bis(3-amino-pyrazine-2-carboxyl-ato-κ2 N(1) O)di-aqua-nickel(II) dihydrate. *Acta Crystallogr. Sect. E* **2013**, *69*, m309–m310. [CrossRef] [PubMed]

37. Koleša-Dobravc, T.; Maejima, K.; Yoshikawa, Y.; Meden, A.; Yasui, H.; Perdih, F. Vanadium and zinc complexes of 5-cyanopicolinate and pyrazine derivatives: Synthesis, structural elucidation and in vitro insulino-mimetic activity study. *New J. Chem.* **2017**, *41*, 735–746. [CrossRef]

38. Benhamada, N.; Bouchene, R.; Bouacida, S.; Zouchoune, B. Molecular structure, bonding analysis and redox properties of transition metal–Hapca [bis(3-aminopyrazine-2-carboxylic acid)] complexes: A theoretical study. *Polyhedron* **2015**, *91*, 59–67. [CrossRef]

39. Dehghanpour, S.; Jahani, K.; Mahmoudi, A.; Babakhodaverdi, M.; Notash, B. In situ hydrothermal synthesis of 2D mercury(I)–organic framework from 3-aminopyrazine-2-carboxylic acid and mercury(II) acetate. *Inorg. Chem. Commun.* **2012**, *25*, 79–82. [CrossRef]

40. Desiraju, G.R.; Ho, P.S.; Kloo, L.; Legon, A.C.; Marquardt, R.; Metrangolo, P.; Politzer, P.; Resnati, G.; Rissanen, K. Definition of the halogen bond (IUPAC Recommendations 2013). *Pure Appl. Chem.* **2013**, *85*, 1711–1713. [CrossRef]

41. Cavallo, G.; Metrangolo, P.; Milani, R.; Pilati, T.; Priimagi, A.; Resnati, G.; Terraneo, G. The Halogen Bond. *Chem. Rev.* **2016**, *116*, 2478–2601. [CrossRef]

42. Gilday, L.C.; Robinson, S.W.; Barendt, T.A.; Langton, M.J.; Mullaney, B.R.; Beer, P.D. Halogen Bonding in Supramolecular Chemistry. *Chem. Rev.* **2015**, *115*, 7118–7195. [CrossRef]

43. Troff, R.W.; Mäkelä, T.; Topić, F.; Valkonen, A.; Raatikainen, K.; Rissanen, K. Alternative Motifs for Halogen Bonding. *Eur. J. Org. Chem.* **2013**, *2013*, 1617–1637. [CrossRef]

44. Rissanen, K. Halogen bonded supramolecular complexes and networks. *CrystEngComm* **2008**, *10*, 1107–1113. [CrossRef]

45. Bui, T.T.T.; Dahaoui, S.; Lecomte, C.; Desiraju, G.R.; Espinosa, E. The Nature of Halogen···Halogen Interactions: A Model Derived from Experimental Charge-Density Analysis. *Angew. Chem. Int. Ed.* **2009**, *48*, 3838–3841. [CrossRef] [PubMed]

46. Metrangolo, P.; Resnati, G. Type II halogen···halogen contacts are halogen bonds. *IUCrJ* **2014**, *1*, 5–7. [CrossRef] [PubMed]

47. Awwadi, F.F.; Willett, R.D.; Peterson, K.A.; Twamley, B. The Nature of Halogen···Halogen Synthons: Crystallographic and Theoretical Studies. *Chem. A Eur. J.* **2006**, *12*, 8952–8960. [CrossRef] [PubMed]

48. Brammer, L.; Minguez Espallargas, G.; Adams, H. Involving metals in halogen-halogen interactions: Second-sphere Lewis acid ligands for perhalometallate ions (M-X···X′-C). *CrystEngComm* **2003**, *5*, 343–345. [CrossRef]

49. Von Essen, C.; Rissanen, K.; Puttreddy, R. Halogen Bonds in 2,5-Dihalopyridine-Copper(I) Halide Coordination Polymers. *Materials* **2019**, *12*, 3305. [CrossRef]

50. Puttreddy, R.; von Essen, C.; Peuronen, A.; Lahtinen, M.; Rissanen, K. Halogen bonds in 2,5-dihalopyridine-copper(ii) chloride complexes. *CrystEngComm* **2018**, *20*, 1954–1959. [CrossRef]

51. Puttreddy, R.; von Essen, C.; Rissanen, K. Halogen Bonds in Square Planar 2,5-Dihalopyridine–Copper(II) Bromide Complexes. *Eur. J. Inorg. Chem.* **2018**, *2018*, 2393–2398. [CrossRef]

52. Puttreddy, R.; Peuronen, A.; Lahtinen, M.; Rissanen, K. Metal-Bound Nitrate Anion as an Acceptor for Halogen Bonds in Mono-Halopyridine-Copper(II) Nitrate Complexes. *Cryst. Growth Des.* **2019**, *19*, 3815–3824. [CrossRef]

53. Kwak, S.H.; Lee, G.-H.; Gong, Y.-D. Synthesis of N-Substituted-2-Aminothiazolo[4,5-b]pyrazines by Tandem Reaction of o-Aminohalopyrazines with Isothiocyanates. *Bull. Korean Chem. Soc.* **2012**, *33*. [CrossRef]

54. Caldwell, J.J.; Veillard, N.; Collins, I. Design and synthesis of 2(1H)-pyrazinones as inhibitors of protein kinases. *Tetrahedron* **2012**, *68*, 9713–9728. [CrossRef]

55. Bartolomé-Nebreda, J.M.; Delgado, F.; Martín-Martín, M.L.; Martínez-Viturro, C.M.; Pastor, J.; Tong, H.M.; Iturrino, L.; Macdonald, G.J.; Sanderson, W.; Megens, A.; et al. Discovery of a Potent, Selective, and Orally Active Phosphodiesterase 10A Inhibitor for the Potential Treatment of Schizophrenia. *J. Med. Chem.* **2014**, *57*, 4196–4212. [CrossRef] [PubMed]

56. Reader, J.C.; Matthews, T.P.; Klair, S.; Cheung, K.-M.J.; Scanlon, J.; Proisy, N.; Addison, G.; Ellard, J.; Piton, N.; Taylor, S.; et al. Structure-Guided Evolution of Potent and Selective CHK1 Inhibitors through Scaffold Morphing. *J. Med. Chem.* **2011**, *54*, 8328–8342. [CrossRef] [PubMed]

57. Hutchings, M.G.; Meyrick, B.H.; Nelson, A.J. Colour and constitution of azo compounds derived from diaminoazines. *Tetrahedron* **1984**, *40*, 5081–5088. [CrossRef]

58. Miesel, J.L. Novel 1-(mono-o-substituted benzoyl)-3-(substituted pyrazinyl) ureas. US Patent No. 4,293,552, 31 July 1979.

59. Massaux, P.M.; Bernard, M.J.; Le Bihan, M.-T. Etude Structurale de CuBr.CH$_3$CN. *Acta Cryst.* **1972**, *B27*, 2419–2424. [CrossRef]

60. Rigaku Oxford Diffraction. *CrysAlisPro Version 38.46*; Rigaku: Tokyo, Japan, 2018.

61. Bruker AXS Inc. COLLECT. In *Bruker AXS BV, 1997-2004*; Bruker AXS Inc.: Madison, WI, USA.

62. Otwinowski, Z.; Minor, W. Processing of X-ray diffraction data collected in oscillation mode. *Methods Enzymol.* **1997**, *276*, 307–326. [CrossRef]

63. Sheldrick, G.M. *SADABS. Program for Empirical Absorption Correction*; University of Göttingen: Göttingen, Lower Saxony, Germany, 1996.

64. Sheldrick, G.M. Crystal structure refinement with SHELXL. *Acta Cryst.* **2015**, *C71*, 3–8. [CrossRef]

65. Dolomanov, O.V.; Bourhis, L.J.; Gildea, R.J.; Howard, J.A.K.; Puschmann, H.J.J. OLEX2: A complete structure solution, refinement and analysis program. *J. Appl. Cryst.* **2009**, *42*, 339–341. [CrossRef]

66. Gruene, T.; Hahn, H.W.; Luebben, A.V.; Meilleur, F.; Sheldrick, G.M.J. Refinement of macromolecular structures against neutron data with SHELXL2013. *Appl. Cryst.* **2014**, *47*, 462–466. [CrossRef]

67. Degen, T.; Sadki, M.; Bron, E.; König, U.; Nénert, G. The HighScore suite. Powder Diffraction (Supplement S2). 20 December 2014; 29, S13–S18.

68. Pawley, G.S. Unit-cell refinement from powder diffraction scans. *J. Appl. Cryst.* **1981**, *14*, 357–361. [CrossRef]

69. Mailman, A.; *unpublished results:* A preliminary structure of the CuBr$_2$ complex of 2-amino-5-chloropyrazine (**2**), *i.e.* **2**·CuBr$_2$ has been determined by single crystal X-ray diffraction methods: Triclinic, *P-1, a* = 6.002(5), 7.078 (5), 8.467 (7), α = 94.225 (6), β =97.238(7) γ = 102.105(7), V = 347.03 Å^3.

70. Kochi, J.K. The Reduction of Cupric Chloride by Carbonyl Compounds. *J. Am. Chem. Soc.* **1955**, *77*, 5274–5278. [CrossRef]

71. Yamada, Y.; Ohba, H.; Noboru, Y.; Daicho, S.; Nibu, Y. Solvation Effect on the NH Stretching Vibrations of Solvated Aminopyrazine, 2-Aminopyridine, and 3-Aminopyridine Clusters. *J. Phys. Chem. A* **2012**, *116*, 9271–9278. [CrossRef] [PubMed]

72. Peng, R.; Li, M.; Li, D. Copper(I) halides: A versatile family in coordination chemistry and crystal engineering. *Coord. Chem. Rev.* **2010**, *254*, 1–18. [CrossRef]

73. Knorr, M.; Bonnot, A.; Lapprand, A.; Khatyr, A.; Strohmann, C.; Kubicki, M.M.; Rousselin, Y.; Harvey, P.D. Reactivity of CuI and CuBr toward Dialkyl Sulfides RSR: From Discrete Molecular Cu4I4S4 and Cu8I8S6 Clusters to Luminescent Copper(I) Coordination Polymers. *Inorg. Chem.* **2015**, *54*, 4076–4093. [CrossRef] [PubMed]

74. Harisomayajula, N.V.S.; Makovetskyi, S.; Tsai, Y.-C. Cuprophilic Interactions in and between Molecular Entities. *Chem. A Eur. J.* **2019**, *25*, 8936–8954. [CrossRef] [PubMed]

75. Barclay, T.M.; Cordes, A.W.; Oakley, R.T.; Preuss, K.E.; Zhang, H. 2,5-Diamino-3,6-dichloropyrazine. *Acta Crystallogr. Sect. C* **1998**, *54*, 1018–1019. [CrossRef]

76. Chao, M.; Schempp, E.; Rosenstein, R.D. Aminopyrazine. *Acta Crystallogr. Sect. B* **1976**, *32*, 288–290. [CrossRef]

77. Näther, C.; Greve, J.; Jeß, I. Synthesis, crystal structures and thermal properties of new copper(I) halide coordination polymers. *Solid State Sci.* **2002**, *4*, 813–820. [CrossRef]

78. Conesa-Egea, J.; Gallardo-Martínez, J.; Delgado, S.; Martínez, J.I.; Gonzalez-Platas, J.; Fernández-Moreira, V.; Rodríguez-Mendoza, U.R.; Ocón, P.; Zamora, F.; Amo-Ochoa, P. Multistimuli Response Micro- and Nanolayers of a Coordination Polymer Based on Cu2I2 Chains Linked by 2-Aminopyrazine. *Small* **2017**, *13*, 1700965. [CrossRef]